

# Polyethylene Glycol - Functionalized Titanium Dioxide Nanoparticles for Extended Release of Diethylenetriaminepentaacetic Acid into Lung Fluid to Enhance the Decorporation of Radioactive Actinides

Almalki M<sup>1</sup>, Lai EPC<sup>1\*</sup>, Ko R<sup>2</sup> and Li CS<sup>2</sup>

<sup>1</sup>Department of Chemistry, Carleton University, Canada

<sup>2</sup>Radiation Protection Bureau, Health Canada, Canada

## Abstract

Titanium dioxide (TiO<sub>2</sub>) nanoparticles have been used widely as a nanocarrier in drug delivery systems due to their high delivery efficiency and controlled release of therapeutic drugs. Diethylenetriaminepentaacetic Acid (DTPA) is an attractive decorporation agent that can enhance the excretion of radioactive actinides such as uranium, plutonium and americium after a radiological incident. However, DTPA is excreted in a short period of time after administration. In this project, biocompatible Polyethylene Glycol (PEG) functionalized TiO<sub>2</sub> nanoparticles was used to load DTPA to increase its residence time in the human body. The prepared DTPA-loaded PEG-functionalized TiO<sub>2</sub> nanoparticles were characterized by transmission electron microscopy, Fourier transform infrared spectroscopy and dynamic light scattering. The prolonged retention of DTPA from PEG-functionalized TiO<sub>2</sub> nanoparticles were also evaluated via dialysis experiments. Liquid chromatography-mass spectrometry analysis of the dialysates showed an extended release of DTPA into simulated lung fluid. This approach was used for the first time to sustain the release of DTPA in an *in vitro* study.

**Keywords:** Decorporation agent; Dialysis; DTPA; *In vitro* release; Simulated lung fluid; Titanium dioxide nanoparticles

**\*Corresponding author:** Edward PC Lai, Department of Chemistry, Carleton University, 1125 Colonel By Drive, Ottawa, ON K1S 5B6, Canada, Tel: +1 61352026003835; E-mail: edward.lai@carleton.ca

**Received Date:** May 06, 2017

**Accepted Date:** August 21, 2017

**Published Date:** September 05, 2017

**Citation:** Almalki M, Lai EPC, Ko R, Li CS (2017) Polyethylene Glycol - Functionalized Titanium Dioxide Nanoparticles for Extended Release of Diethylenetriaminepentaacetic Acid into Lung Fluid to Enhance the Decorporation of Radioactive Actinides. J Nanosci Nanomed Nanobio 1: 002.

## Introduction

During radiological accidents, inhalation of radioactive materials could be the main route of internal contamination [1]. During the radioactive decay harmful ionizing radiation, such as alpha particles, beta particles, and gamma rays are emitted [2]. The quantity of radionuclides inhaled, the type of radiation, and the proximity of contamination to organs in the human body determine the degree of hazard. Cellular exposure to ionizing radiation leads to the generation of Reactive Oxygen Species (ROS) that can damage biological macromolecules via the radiolysis of intracellular H<sub>2</sub>O [3-5].

To reduce the ionization radiation damage to the human body systems, chelation therapy may be required. Chelation, also called decorporation, is referring to the removal of internal radioactive contaminants from the body following a radiological incident. Diethylenetriaminepentaacetic Acid (DTPA) is recognized as a chelating agent that accelerates the excretion of actinides. It works best when given shortly after radioactive isotopes enter the body. DTPA comes in three forms: calcium DTPA, zinc DTPA and sodium DTPA. All forms are very effective in enhancing the elimination of actinides such as

plutonium and americium [6]. DTPA catches these radionuclides in the body and turns them into a stable coordination complex form that can be excreted in the urine [7]. The efficacy of DTPA as a decorporation agent is limited by several factors. DTPA exhibits low distribution in tissues due to its low solubility. Therefore, it can only chelate contaminants that are still in the blood or extracellular fluid. Moreover, it has a residence time as short as 90 minutes in humans due to fast clearance mechanisms [8]. Therefore repeated daily doses over several weeks may be required to achieve the desired decorporation. However, such a frequent dosage of DTPA can cause severe toxic effects by the depletion of essential elements such as magnesium, manganese and even calcium or zinc [9].

Systemic delivery of DTPA has traditionally been used for the decorporation of radioactive contaminants. However, due to its low local concentration in the lungs, the clinical application remains largely unsatisfactory for treating contamination via inhalation [10]. Achieving a sustained presence of the chelating agent in the lungs is very challenging [11]. Drug delivery to the lungs through inhalation is considered to be particularly advantageous due to a high-localized concentration of the agent and relatively low side effects [12].

Nanoparticles, also known as ultrafine particles, come together to compose what is known as Nanomaterials (NMs). The physicochemical properties of nanoparticles are dependent on their particle size, chemical composition, electronic charge, surface structure, crystalline phase, solubility, shape and aggregation [13]. Nanotechnology has emerged as a highly valuable, useful and versatile technology. It has found application in catalysis, cosmetics, drug carriers, food additives

and sunscreen. Complimentary to the development of nanotechnology, Drug Delivery Nanosystems (DDNSs) is gaining more attention by researchers and scientists worldwide [14-16]. Among NMs, Titanium dioxide Nanoparticles ( $\text{TiO}_2$  NPs) are one of the most used drug delivery Nanosystems [17].  $\text{TiO}_2$  has been used as a drug carrier for various drugs such as daunorubicin, sodium phenytoin, temozolomide and valproic acid.  $\text{TiO}_2$  showed high delivery efficiency and sustained drug release over days, weeks, or months. This can decrease the exposure time to the drug which lead to less side effect [18-21].

Many industries make use of  $\text{TiO}_2$  NPs and can be found in food products, various medicines and as well as cosmetics [22-24].  $\text{TiO}_2$  NPs efficacy can be attributed to their ability to reach various parts of the body. This can be accomplished through exposure routes, which include inhalation, ingestion and gastrointestinal tract absorption [25]. DDNSs have a unique potential to not only enhance drug bio-availability, but also to extend the period of drug release and enhance the drug targeting [26].

Polyethylene Glycol (PEG) is a polyether compound with many medical applications due to its biocompatible and biodegradable properties [27]. The attachment of PEG to the surface of nanoparticles increases their biocompatibility [28]. Jugan et al., and Yaling et al., performed a study on the influence of  $\text{TiO}_2$  nanoparticles on human lung cells and mouse liver cells [29]. This study confirmed that the toxicity of  $\text{TiO}_2$  is reduced when functionalized with polymers [30]. Nanoparticles that are not functionalized with PEG are recognized as foreign products and ejected from the blood circulation by macrophage cells that exist within the reticuloendothelial system. The  $\text{TiO}_2$  nanocarrier has been used successfully for the controlled release of anticancer drugs such as paclitaxel [31,32].

In this study, we loaded DTPA onto PEG-functionalized  $\text{TiO}_2$  nanoparticles in order to achieve effective delivery and sustained release of this agent into the lungs. The prepared DTPA-loaded PEG-functionalized  $\text{TiO}_2$  NPs were characterized by different analytical techniques. To confirm our hypothesis of extended release, DTPA released from the PEG- $\text{TiO}_2$  into simulated lung fluid was monitored via dialysis experiments. The loading capacity of DTPA on PEG-functionalized  $\text{TiO}_2$  NPs was determined by LC-MS analysis.

## Materials and Methods

Titanium dioxide nanoparticles (20 nm), polyethylene glycol (molecular weight or degree of polymerization Mn6000), Diethylenetriaminepentaacetic Acid ( $\text{DTPA-H}_5$ ), penta sodium salt of diethylenetriaminepentaacetic Acid ( $\text{DTPA-Na}_5$ ), calcium chloride, iron (III) chloride hexahydrate, magnesium chloride, potassium chloride, sodium chloride, sodium citrate dehydrate, sodium hydrogen carbonate, sodium sulfate, dihydrate sodium acetate, disodium hydrogen phosphate, D-mannitol and formic acid were purchased from Sigma-Aldrich and are ACS grade or greater. Regenerated cellulose dialysis membranes (MWCO 3500 D) were purchased from Thermo Fisher Scientific.

## Absorption Test of $\text{DTPA-Na}_5$ /DT- $\text{PA-H}_5$ into PEG Functionalized $\text{TiO}_2$ NPs

A solution of  $\text{DTPA-Na}_5$  (1 mL, 1000 mg/L) was mixed with different concentrations of PEG-functionalized  $\text{TiO}_2$  nanoparticles (0.0.0058, 0.0233, 0.0583 and 0.175 g/mL) and adjusted to final volumes of 1.5 mL. Also, another solution of  $\text{DTPA-H}_5$  (1 mL, 1000 mg/L) was mixed with a new batch of PEG-functionalized  $\text{TiO}_2$  nanoparticles in the same aforementioned concentrations [33]. The mixtures were left overnight to interact followed by centrifugation at 4500 rpm for 1 h at 18°C. Liquid Chromatography-Mass Spectrometry (LC-MS) analysis of the supernatants was performed to determine any free DTPA.

## Preparation of $\text{DTPA-H}_5$ -PEG Functionalized $\text{TiO}_2$

$\text{TiO}_2$  nanoparticles (20 nm) were mixed with 1% Polyethylene Glycol (PEG) solution in distilled deionized water, and the mixture was magnetically stirred overnight. The resulting PEG-functionalized  $\text{TiO}_2$  were collected by centrifugation at 4500 rpm for 1 h at 18°C, and washed with water [31,32]. Similarly, Polyethylenimine (PEI)-functionalized  $\text{TiO}_2$  nanoparticles were prepared. An aqueous solution of DTPA at 1 mg/mL was added into the PEG-functionalized  $\text{TiO}_2$  and the mixture was magnetically stirred overnight. The DTPA loaded PEG functionalized  $\text{TiO}_2$  nanoparticles were separated by centrifugation at 4500 rpm for 1 h at 18°C, washed with distilled water for freeze-drying [31,32]. A pre-frozen solution of DTPA loaded PEG functionalized  $\text{TiO}_2$  was mixed with a 5% solution of D-mannitol before freeze-drying in a Labconco model 7753020 freeze dryer operating at a temperature of -53°C<sup>7</sup>. Mannitol was used as a dispersant to prevent the aggregation of DTPA loaded PEG functionalized  $\text{TiO}_2$  during the freeze-drying process. DTPA-loaded PEG-functionalized  $\text{TiO}_2$  nanoparticles were obtained as dry powders.

## Characterization of Nanoparticles by Transmission Electron Microscopy

Transmission Electron Microscopy (TEM) was used to characterize the  $\text{TiO}_2$  nanoparticles, before and after functionalization with PEG and loading of DTPA on a FEI Tecnai G2 F20 microscope operating at 200 kV.

## Characterization of Nanoparticles by Fourier Transforms Infrared Spectroscopy

The chemical structures of  $\text{TiO}_2$  nanoparticles and surface modified nanoparticles were characterized using an ABB (Bomem MB series, Quebec, Canada) Fourier Transform Infrared (FTIR) spectrometer. Disc samples were prepared by grinding 2 mg of nanoparticles with 200 mg of spectrophotometric-grade KBr. All FTIR spectra were obtained in the spectral region of 600-4000  $\text{cm}^{-1}$ .

## Characterization of Nanoparticles by Dynamic Light Scattering

Dynamic Light Scattering (DLS) was used to measure the hydrodynamic size distribution of  $\text{TiO}_2$  nanoparticles and DTPA loaded PEG- $\text{TiO}_2$  nanoparticles suspended in 10 mM potassium nitrate buffer. DLS analysis of each suspension was performed using a Brookhaven Instruments nano DLS particle size analyzer (Holtville, NY, USA). Each suspension was measured in ten replicates of 10 s each for higher accuracy [7,34].

## Loading Capacity of PEG-Functionalized $\text{TiO}_2$

The prepared PEG-functionalized  $\text{TiO}_2$  nanoparticles at different concentrations 0.0084, 0.0168, 0.0252, 0.0336, 0.042, 0.084, 0.126 and 0.168 g/mL were mixed with 1 mL of DTPA- $\text{H}_3$  at 1000 mg/L. The mixtures were left overnight to interact followed by centrifugation. LC-MS analysis of the supernatants was performed to determine the PEG- $\text{TiO}_2$  capacity. The capacity of polyethylenimine functionalized  $\text{TiO}_2$  nanoparticles (PEI- $\text{TiO}_2$ ) was determined following the same procedure [33].

## In vitro Release of DTPA Loaded PEG-Functionalized $\text{TiO}_2$ Nanoparticles

Simulated Lung Fluid (SLF) was prepared with pH 7.4 for *in vitro* release tests based on Marques et al., description (Gamble's solution) [35]. DTPA loaded PEG-functionalized  $\text{TiO}_2$  nanoparticles were dispersed in 10mL of SLF, followed by transferring to dialysis membrane tubing (MWCO 3500). Then, the dialysis tubing was immersed in a beaker containing 50 mL of lung fluid. The dialysis process was performed at  $37 \pm 1^\circ\text{C}$  under magnetic stirring. At appropriate time intervals, a dialysate sample was taken and replaced by the same volume of SLF to keep the dialysis volume constant. The *in vitro* release test was conducted for 28-50 hours. Finally, all the dialysate samples were analyzed by LC-MS/MS to determine the concentration of released DTPA versus the dialysis time.

## Determination of DTPA Concentration by Liquid Chromatography-tandem Mass Spectrometry

Liquid Chromatography-tandem Mass Spectrometry (LC-MS/MS) was used to determine the DTPA concentration released during the dialysis experiments. DTPA standard solutions and dialysate samples were mixed with  $\text{Fe}^{3+}$  ions to form a stable  $[\text{M}-4\text{H}^+ + \text{Fe}^{3+}]^-$  cluster ion. All Fe-DTPA standards and dialysate samples were diluted with 1:1 ratio of 0.1% formic acid before the analysis. A C18 column was used in LC (50 mm x 2.1 mm) maintained at room temperature. The mobile phase was prepared by mixing 98% A and 2% B at a flow rate of 0.4 mL/min: (A) 0.1% formic acid in ultrapure water and (B) 0.1% formic acid in acetonitrile. Formic acid facilitated the formation of protonated ions for higher MS detection sensitivity. Mass spectrometric

analysis was performed using an Agilent Technologies model 6460 triple quad MS/MS system that was equipped with an ESI source operating in the negative mode. The operating parameters were: nitrogen gas flow rate = 9.8 L/min, gas temperature =  $300^\circ\text{C}$ , nebulizer pressure = 15 psi, capillary voltage = 4000 V, fragmentor voltage = 135 V, and cell accelerator voltage = 7 V. Single ion monitoring was set up to record the peak at  $m/z = 445$ .

## Results and Discussion

When a solution of DTPA- $\text{Na}_3$  or DTPA- $\text{H}_3$  was added into two batches of PEG-functionalized  $\text{TiO}_2$  NPs, most of the DTPA- $\text{H}_3$  was absorbed into the nanoparticles as indicated by decreases in the DTPA concentration that remained in the supernatant liquid (Figure 1). However, all the DTPA- $\text{Na}_3$  was found to remain in the supernatant liquid as illustrated in Figure 2. No change in the DTPA concentration was observed even with 1 week of contact time with varying amounts of functionalized NPs. Samples prepared with the addition of DTPA- $\text{H}_3$  to the functionalized  $\text{TiO}_2$  NPs showed a significant decrease in the DTPA peak area as the concentration of PEG- $\text{TiO}_2$  nanoparticles increased. The latter result suggested strong binding of DTPA- $\text{H}_3$  with PEG-functionalized  $\text{TiO}_2$  NPs compared to DTPA- $\text{Na}_3$ . The formation of hydrogen bonds was a key factor for the interaction between DTPA- $\text{H}_3$  and PEG. The ability of DTPA- $\text{H}_3$  to act as a hydrogen donor allows the formation of hydrogen bonds between its carboxylic acid groups and the hydroxyl groups of PEG. This can explain the higher absorption of DTPA- $\text{H}_3$  into the PEG-functionalized  $\text{TiO}_2$  compared to DTPA- $\text{Na}_3$ . Moreover, the low absorption of DTPA- $\text{Na}_3$  could be due to the high affinity of DTPA $^{5-}$  toward  $\text{Na}^+$  ions compared to PEG. Kubota et al., found that DTPA in its acidic form was retained in the blood circulation for a longer time compared to its salt forms which were excreted very fast via urine [36]. Based on this result; DTPA- $\text{H}_3$  has been used for further experiments.

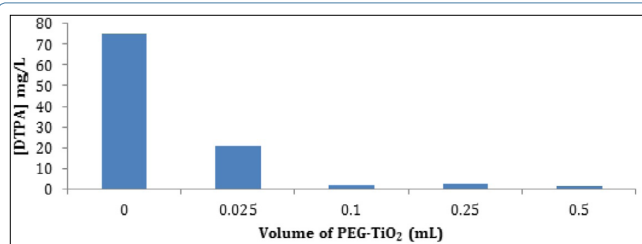


**Figure 1:** Absorption test of DTPA- $\text{H}_3$  into PEG-functionalized  $\text{TiO}_2$  nanoparticles by monitoring the concentration of DTPA remaining in the supernatant liquid.

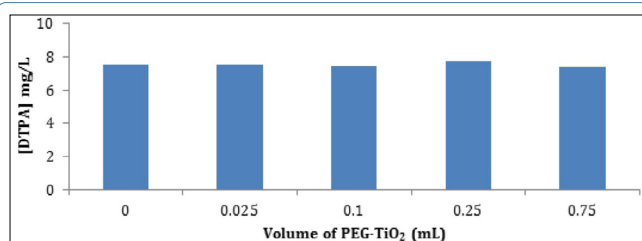


**Figure 2:** Absorption test of DTPA- $\text{Na}_3$  into PEG-functionalized  $\text{TiO}_2$  nanoparticles by monitoring the concentration of DTPA remaining in the supernatant liquid.

The TEM images in Figure 3 show an average particle size of 17-21 nm for  $\text{TiO}_2$  nanoparticles and 37 nm for DTPA loaded PEG-functionalized  $\text{TiO}_2$ . This increase in size could be attributed to DTPA loading and PEG fictionalization of  $\text{TiO}_2$  NPs. Energy Dispersion x-ray (EDX) has been used to confirm our results. The atomic



percentage of C increased in the DTPA loaded PEG-functionalized TiO<sub>2</sub> nanoparticles when compared to the PEG-functionalized TiO<sub>2</sub> nanoparticles before DTPA loading.

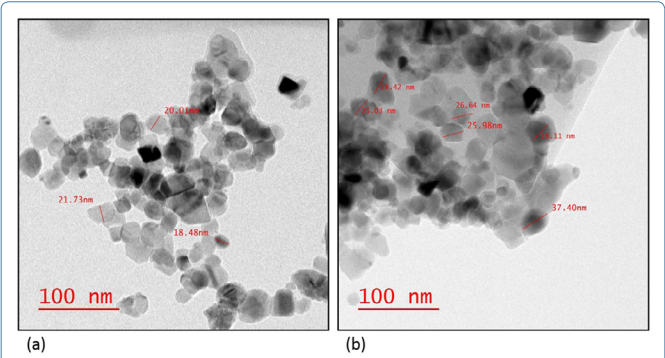


**Figure 3:** TEM images: (a) TiO<sub>2</sub> nanoparticles, and (b) DTPA-loaded PEG-functionalized TiO<sub>2</sub> nanoparticles. The TEM instrument offers a point resolution of 0.27 nm and a magnification ranging from 21 x to 700,000x.

Figure 4 exhibits the FTIR of TiO<sub>2</sub>, DTPA, PEG and DTPA loaded PEG functionalized TiO<sub>2</sub>. The presence of characteristic absorption peaks of the TiO<sub>2</sub>, PEG and DTPA in the DTPA loaded PEG functionalized TiO<sub>2</sub> suggested the loading of DTPA into the PEG functionalized NPs. The band at 602 cm<sup>-1</sup> in the TiO<sub>2</sub> (4a) corresponds to TiO<sub>2</sub> stretching vibration, shifted into 707 cm<sup>-1</sup> in the DTPA loaded PEG functionalized TiO<sub>2</sub> (4d). The intense band in the PEG at 2889 cm<sup>-1</sup> (4c) which, corresponds to the C-H stretching vibrations, shifted into 2866 cm<sup>-1</sup> in the DTPA loaded PEG functionalized NPs. The bands in the DTPA (4b) that appears at 1733 and 1698 cm<sup>-1</sup>, corresponding to the COO<sup>-</sup> and C=O functional groups respectively, are shifted to 1728 and 1636 cm<sup>-1</sup> in the DTPA loaded PEG functionalized TiO<sub>2</sub>.

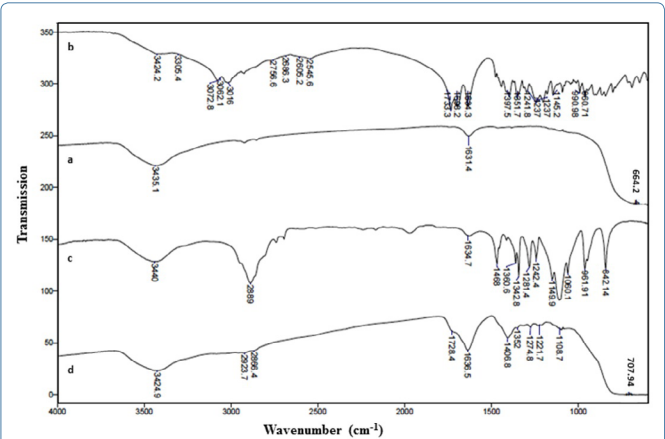


**Figure 4:** FTIR spectra: (a) TiO<sub>2</sub> nanoparticles, (b) PEG, (c) DTPA, and (d) DTPA-loaded PEG-functionalized TiO<sub>2</sub> nanoparticles.

Dynamic light scattering of the TiO<sub>2</sub>NPs exhibited a hydrodynamic diameter of 66 nm. The DTPA loaded PEG-TiO<sub>2</sub> showed a significant increase in their hydrodynamic diameter compared to the bare TiO<sub>2</sub> NPs. This increase confirmed the successful formation of DTPA-loaded PEG-functionalized TiO<sub>2</sub>nanoparticles.

The binding capacity experiment in Figure 4 showed a decrease in the DTPA peak area as the PEG functionalized TiO<sub>2</sub> NPs concentration increased from 0.0056 to 0.028 g/mL. The DTPA concentrations in the supernatant decrease, which means more DTPA, have been absorbed into the surface of PEG-TiO<sub>2</sub>. However, no significant change in the absorption was observed when the PEG-functionalized

TiO<sub>2</sub> concentration increased from 0.056, to 0.084 g/mL indicating equilibrium has been reached (Figure 5a). The capacity of PEG-functionalized TiO<sub>2</sub> nanoparticles was determined to be 21 mg DTPA/g of PEG-TiO<sub>2</sub> NPs based on LC-MS analysis. The low capacity of the functionalized TiO<sub>2</sub> is due to the polymer fictionalization into the NPs surface. However, the use of coating polymer was essential for the reduction of TiO<sub>2</sub> nanoparticles toxicity and clearance by macrophage system. To increase the loading capacity of PEG-functionalized TiO<sub>2</sub> NPs, TiO<sub>2</sub> were functionalized with various 2%, 3% and 4% concentrations of PEG. However, the resulted PEG-functionalized TiO<sub>2</sub> NPs didn't exhibit higher capacity than the NPs that functionalized with 1% PEG concentration. In an attempt to improve the loading capacity of functionalized TiO<sub>2</sub> nanoparticles, Polyethylenimine (PEI) was used to functionalize the TiO<sub>2</sub> surface in a similar way to PEG. Theoretically PEI is a positively charged polymer at neutral pH. Therefore, electrostatic attractions between PEI and negatively charged DTPA could be strong compared to the electrostatic repulsion for negatively charged PEG. This can lead to more loading of DTPA into the PEI-functionalized TiO<sub>2</sub> nanoparticles. However, PEI-functionalized TiO<sub>2</sub> nanoparticles did not exhibit efficient loading of DTPA compared to PEG-functionalized TiO<sub>2</sub> nanoparticles, as shown in Figure 5b. About 50% of the DTPA was initially absorbed into the PEI-functionalized TiO<sub>2</sub> nanoparticles at 0.0056 g/mL. When more PEI-functionalized TiO<sub>2</sub> nanoparticles were added from 0.0112 g/mL up to 0.084 g/mL, the concentration of DTPA only decreased slightly, corresponding to a modest increase in DTPA loading from 21 mg/g to 25 mg DTPA/g of PEI-functionalized TiO<sub>2</sub> nanoparticles. Hence, the DTPA encapsulation efficiency of PEI-functionalized TiO<sub>2</sub> nanoparticles is not as good as PEG-functionalized TiO<sub>2</sub> nanoparticles. Neither PEG-TiO<sub>2</sub> nor PEI-TiO<sub>2</sub> nanoparticles showed any affinity toward gadolinium Gd<sup>3+</sup>, which had previously been used as a model trivalent ion. Therefore, decorporation of radioactive actinides will rely totally on the loaded DTPA when these functionalized TiO<sub>2</sub> nanoparticles are introduced to the contaminated lungs [37].

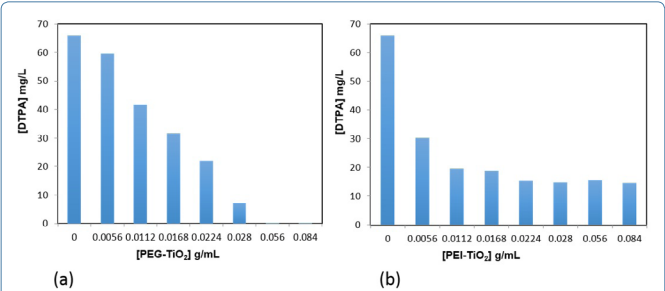


**Figure 5:** DTPA-H<sub>3</sub> binding capacities: (a) PEG-functionalized TiO<sub>2</sub> nanoparticles; (b) PEI-functionalized TiO<sub>2</sub> nanoparticles.

## Drug Release Profile

DTPA has high affinity toward trivalent ions that are present in the lung fluid. This can lead to the formation of several DTPA complexes. Therefore, the released DTPA in the dialysate samples was determined by LC-MS upon the formation of a stable Fe-DTPA<sup>2-</sup> complex due to the highest affinity of DTPA<sup>5-</sup> towards the Fe<sup>3+</sup> metal ion compared to various metal ions such as Ca<sup>2+</sup>, Cd<sup>2+</sup>, Co<sup>2+</sup>, Cu<sup>2+</sup>, Mn<sup>2+</sup> and Zn<sup>2+</sup> [38,39]. As shown in Figure 6a, the Fe-DTPA<sup>2-</sup> peak appeared at a short retention time of 0.555 minutes. A linear trend line equation obtained by running a series of Fe-DTPA standard solutions was used to determine the unknown DTPA concentration in each dialysate as shown in Figure 6b.

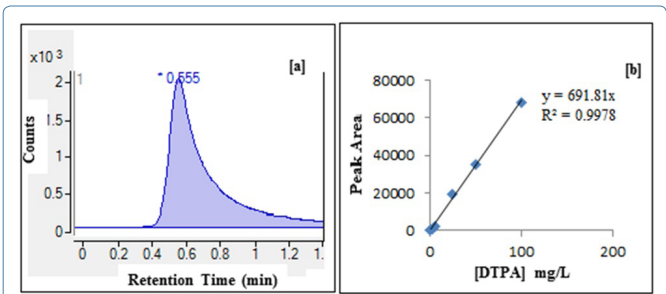


**Figure 6:** (a) Liquid chromatogram of Fe-DTPA<sup>2-</sup> at a retention time of 0.555 min using selected ion monitoring at  $m/z = 445$ . (b) Standard calibration curve of Fe-DTPA<sup>2-</sup> peak areas versus DTPA concentrations.

The drug release profile of DTPA from PEG functionalized titanium dioxide nanoparticles into simulated lung fluid is given in Figure 7. The drug release profiles exhibit a rapid release of drug in the initial stage, followed by a slow, steady and controlled release of drug. Drug release profile (27 mg of DTPA in 950 mg of PEG-TiO<sub>2</sub>) shows 88% release of DTPA occurs around 22 hours and time for half release was 4 hours. The obtained drug release half-life is longer than the biological half-life of DTPA reported in the literature, which is 90 minutes. In the initial stage, the cumulative amounts of DTPA released rapidly reach 12.5 mg/L in the first 3.4 h. The cumulative amounts of DTPA increase slowly to reach 20 mg/L within the next 8 h. At 21 h the accumulative drug released increased from 20 to 25.8 mg/L to reach its maximum concentration. After 21 h there was no significant increase in the cumulative DTPA amounts. Due to this promising result, drug release of DTPA loaded PEG-TiO<sub>2</sub> was performed in the presence of plain DTPA as a control. The plain drug concentration was equal to the concentration of DTPA loaded into the PEG-TiO<sub>2</sub>. The DTPA released from PEG-TiO<sub>2</sub> showed an extended drug release compared to the plain drug. The drug release profile of (70 mg/L of DTPA) shows a complete release of DTPA occurs around 22 h as shown in Figure 8. The 50% of the total DTPA concentration was released from the PEG-TiO<sub>2</sub> at 210 minutes, while 50% of the plain drug released at 150 minutes. The half-life of the drug released from PEG-TiO<sub>2</sub> NPs is 60 minutes longer than the plain drugs' half-life.

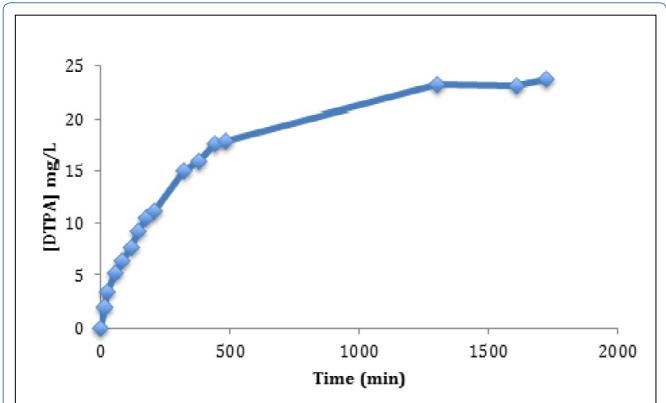


**Figure 7:** Drug release profile of DTPA-loaded PEG-functionalized TiO<sub>2</sub> nanoparticles.

The initial burst release of the drug could be attributed to the DTPA that absorbed into the surface of PEG. Then, the drug molecules that interact strongly or encapsulated into the PEG-TiO<sub>2</sub> are released. In order to improve the drug release, it is very important to understand factors that affect the drug release such as drug solubility, particles size, and polymer-drug interaction [40].

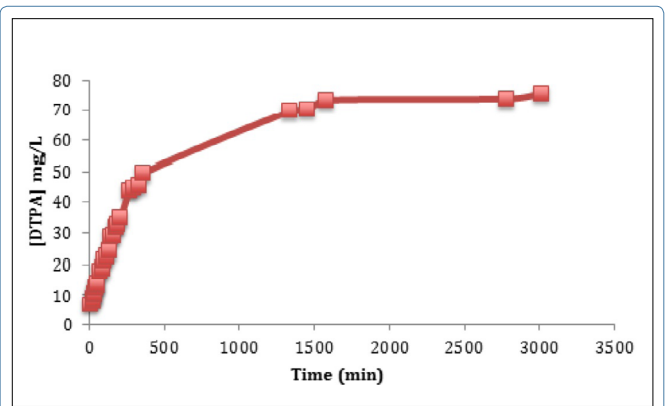


**Figure 8:** Drug release profile of plain DTPA as a control.

## Conclusion

Polyethylene glycol functionalized titanium dioxide nanoparticles have been developed successfully for use as a drug carrier. The loading capacity of DTPA on the prepared PEG-TiO<sub>2</sub> remains lower than the desired for application in decorporation. However, the prepared DTPA loaded PEG-TiO<sub>2</sub> showed a sustained drug release compared to DTPA itself, indicating a promising future for further development. The use of DTPA loaded PEG-functionalized TiO<sub>2</sub> as a decorporation Nanosystems for radioactive contaminants will be tested in the future.

## References

- Fattal E, Tsapis N, Phan G (2015) Novel drug delivery systems for actinides (uranium and plutonium) decontamination agents. *Adv Drug Deliv Rev* 90: 40-54.
- Brandt A, Meeßen J, Jänicke RU, Raguse M, Ott S (2017) Simulated Space Radiation: Impact of Four Different Types of High-Dose Ionizing Radiation on the Lichen. *Astrobiology* 17: 136-144.
- Azzam EI, Jay-Gerin JP, Pain D (2012) Ionizing radiation-induced metabolic oxidative stress and prolonged cell injury. *Cancer Lett* 327: 48-60.
- Panganiban R-AM, Snow AL, Day RM (2013) Mechanisms of radiation toxicity in transformed and non-transformed cells. *Int J Mol Sci* 14: 15931-15958.
- Gebicki JM (2016) Oxidative stress, free radicals and protein peroxides. *Arch Biochem Biophys* 595: 33-39.
- U S Food and Drug Administration (2015) Department of Health and Human Services: Calcium-DTPA and Zinc-DTPA Information Page. U S Food and Drug Administration, Silver Spring, Maryland, USA.
- Chen S, Lai EPC, Ko R, Li CS, Wyatt H (2016) Inhalable Chitosan Triphosphate Nanoparticles for Extended Release of DTPA into Lung Fluid. *Nanomedicine & Nanotechnology Open Access* 1: 000106.
- Aime S, Caravan P (2009) Biodistribution of gadolinium-based contrast agents, including gadolinium deposition. *J MagnReson Imaging*. 30: 1259-1267.
- Sorour MH, Hani HA, Shaalan HF, El-Sayed MMH (2016) Experimental screening of some chelating agents for calcium and magnesium removal from saline solutions. *Desalination and water Treatment* 57 48-49.
- Phan G, Herbert A, Cholet S, Benech H, Deverre JR (2005) Pharmacokinetics of DTPA entrapped in conventional and long-circulating liposomes of different size for plutonium decorporation. *J Control Release* 110: 177-188.

11. Patel A, Woods A, Riffo-Vasquez Y, Babin-Morgan A1, Jones MC, et al. (2016) Lung inflammation does not affect the clearance kinetics of lipid nanocapsules following pulmonary administration. *J Control Release* 235: 24-33.
12. Gervelas C, Serandour AL, Geiger S, Grillon G, Fritsch P, et al. (2007) Direct lung delivery of a dry powder formulation of DTPA with improved aerosolization properties: effect on lung and systemic decorporation of plutonium. *J Control Release* 118: 78-86.
13. Wang A, Marinakos SM, Badireddy AR, Powers CM, Houck KA (2013) Characterization of physicochemical properties of nanomaterials and their immediate environments in high-throughput screening of nanomaterial biological activity. *Wiley Interdiscip Rev Nanomed Nanobiotechnol* 5: 430-448.
14. Choi H, Stathatos E, Dionysiou DD (2006) Sol-gel preparation of mesoporous photocatalytic TiO<sub>2</sub> films and TiO<sub>2</sub>/Al<sub>2</sub>O<sub>3</sub> composite membranes for environmental applications. *Applied Catalysis B: Environmental* 63: 60-67.
15. Aitken RJ, Chaudhry MQ, Boxall AB, Hull M (2006) Manufacture and use of nanomaterials: current status in the UK and global trends. *Occup Med (Lond)* 56: 300-306.
16. Briffa SM, Lynch L, Trouillet V, Bruns M, Hapiuk D, et al. (2017) Development of scalable and versatile nanomaterial libraries for nanosafety studies: polyvinylpyrrolidone (PVP) capped metal oxide nanoparticles. *RSC Adv* 7: 3894-3906.
17. Yin ZF, Wu L, Yang HG, Su YH (2013) Recent progress in biomedical applications of titanium dioxide. *Phys Chem Chem Phys* 15: 4844-4858.
18. Heredia-Cervera BE, González-Azcorra SA, Rodríguez-Gattorno G, López T, Ortiz-Islas E, et al. (2009) Controlled Release of Phenytoin from Nanostructured TiO<sub>2</sub> Reservoir. *Sci Adv Mater* 1: 63-68.
19. Uddin MJ, Mondal D, Morris CA, Lopez T, Diebold U, et al. (2011) An *in vitro* controlled release study of valproic acid encapsulated in a titania ceramic matrix. *Appl Surf Sci* 257: 7920-7927.
20. Qin Y, Sun L, Li X, Cao Q, Wang H, et al. (2011) Highly water-dispersible TiO<sub>2</sub> nanoparticles for doxorubicin delivery: effect of loading mode on therapeutic efficacy. *J Mater Chem* 21: 18003-18010.
21. Wu KC, Yamauchi Y, Hong CY, Yang YH, Liang YH, et al. (2011) Biocompatible, surface functionalized mesoporous titania nanoparticles for intracellular imaging and anticancer drug delivery. *Chem Commun* 47: 5232-5234.
22. Peters RJ, van Bommel G, Herrera-Rivera Z, Helsper HP, Marvin HJ, et al. (2014) Characterization of Titanium Dioxide Nanoparticles in Food Products: Analytical Methods To Define Nanoparticles. *J Agric Food Chem* 62: 6285-6293.
23. Diasanayakea MAK, Senadeeraa GKR, Sarangikaa HNM, Ekanayakea PMPC, Thotawattagea CA, et al. (2016) TiO<sub>2</sub> as a low cost, multi functional material. *Materials Today: Proceedings* 3: 40-47.
24. Kaida T, Kobayashi K, Adachi M, Suzuki F (2004) Optical characteristics of titanium oxide interference film and the film laminated with oxides and their applications for cosmetics. *J Cosmet Sci* 55: 219-220.
25. Shi H, Magaye R, Castranova V, Zhao J (2013) Titanium dioxide nanoparticles: a review of current toxicological data. *Part Fibre Toxicol* 10: 15.
26. Genç L, Kutlu H, Guney G (2015) Vitamin B12-loaded solid lipid nanoparticles as a drug carrier in cancer therapy. *Pharm Dev Technol* 20: 337-344.
27. Gosecki M, Gadzinowski M, Gosecka M, Basinska T, Slomkowski S (2016) Polyglycidol, Its Derivatives, and Polyglycidol-Containing Copolymers-Synthesis and Medical Applications. *Polymers* 8: 227.
28. Sawhney AS, Pathak CP, Hubbell JA (1993) Interfacial photopolymerization of poly(ethylene glycol)-based hydrogels upon alginate-poly(L-lysine) microcapsules for enhanced biocompatibility. *Biomaterials* 14: 1008-1016.
29. Cui Y, Liu H, Zhou M, Duan Y, Li N, et al. (2011) Signaling pathway of inflammatory responses in the mouse liver caused by TiO<sub>2</sub> nanoparticles. *J Biomed Mater Res A* 96: 221-229.
30. Pan Z, Lee W, Slutsky L, Clark RA, Pernodet N, et al. (2009) Adverse effects of titanium dioxide nanoparticles on human dermal fibroblasts and how to protect cells. *Small* 5: 511-520.
31. Venkatasubbu GD, Ramasamy S, Ramakrishnan V, Kumar J (2013) Folate targeted PEGylated titanium dioxide nanoparticles as a nanocarrier for targeted paclitaxel drug delivery. *Advanced Powder Technology* 24: 947-954.
32. Steele TW, Huang CL, Widjaja E, Boey FY, Loo JS, et al. (2011) The effect of polyethylene glycol structure on paclitaxel drug release and mechanical properties of PLGA thin films. *Acta Biomater* 7: 1973-1983.
33. Kataria N, Garg VK, Jain M, Kadirvelu K (2016) Preparation, characterization and potential use of flower shaped Zinc oxide nanoparticles (ZON) for the adsorption of Victoria Blue B dye from aqueous solution. *Adv Powder Technol* 27: 1180-1188.
34. Alsudir S, Lai EPC (2017) Selective detection of ZnO nanoparticles in aqueous suspension by capillary electrophoresis analysis using dithiothreitol and L-cysteine adsorbates. *Talanta* 169: 115-122.
35. Marques MRC, Loebenberg R, Almukainzi M (2011) Simulated Biological Fluids with Possible Application in Dissolution Testing. *Dissolution Technologies* 18: 15-28.
36. Sato H, Kubota Y, Takahashi S, Matsuoka O (1989) Effects of H<sub>5</sub>-DTPA and Ca-DTPA on the Removal of <sup>59</sup>Fe from Rats Injected with <sup>59</sup>Fe-iron Dextran. *Hoken Butsuri* 24: 109-114.
37. Miller SC, Wang X, Bowman B (2010) Pharmacological properties of orally available, amphipathic polyaminocarboxylic acid chelators for actinide decorporation. *Health Phys* 99: 408-412.
38. Zhou S, Zhang B, Sturm E, Teagarden D, Schöneich C (2010) Comparative evaluation of disodium edetate and diethylenetriaminepentaacetic acid as iron chelators to prevent metal -catalyzed destabilization of a therapeutic monoclonal antibody. *J Pharm Sci* 99: 4239-4250.
39. Siepmann F, Muschert S, Flament MP, Leterme P, Gayot A, et al. (2006) Controlled drug release from Gelucire-based matrix pellets: experiment and theory. *Int J Pharm* 317: 136-143.
40. Vora A, Rega A, Dollimore D, Alexander KS (2002) Thermal Stability of folic acid. *Thermochimica Acta* 392: 209-220.